

The influence of various grease compositions and silver nanoparticle additives on electrically induced rolling-element bearing damage

Samuel BOND¹, Robert L. JACKSON^{2,*}, German MILLS¹

¹ Department of Chemistry and Biochemistry, Auburn University, Auburn 36849-5412, USA

² Department of Mechanical Engineering, Auburn University, Auburn 36849-5412, USA

Received: 06 August 2023 / Revised: 16 September 2023 / Accepted: 03 October 2023

© The author(s) 2023.

Abstract: Leakage currents accelerate surface degradation of metal contacts via small scale arcing across lubricating films, but recent observations suggest that metallic nanoparticle additives in lubricants may be useful to improve contact performance. These findings prompted a study that examined electrically induced surface pitting of steel contacts in the presence of several lubricating greases including some containing nanometer-sized colloidal silver (Ag) particles. Reciprocating rolling sphere-on-disk experiments were conducted under electro-tribological loads employing polyurea greases derived from mineral and synthetic base oils with and without additives. Friction forces and electrical resistance were monitored continuously during the tests; surface changes were characterized by means of optical spectroscopy, stylus profilometry, and scanning electron microscopy (SEM) including compositional analysis using energy dispersive spectroscopy (EDS). The observations demonstrate that surface pitting induced by arcing occurs mainly at the points where the rolling motion changes direction and that eroded metal is deposited along the wear groove. Micron-sized pits are formed which contain carbon and oxygen indicating that arcing causes decomposition of the hydrocarbon lubricants. Numerous findings indicate a significant inhibition of pitting is induced by the Ag nanoparticles; some greases containing other additives exhibit a similar, although less pronounced, effect.

Keywords: electric motor bearings; wheel bearings; electric vehicles; arcing; electrically induced bearing damage; pitting; leakage current; stray current

1 Introduction

Electric vehicles continue to grow in usage which also brings into focus their tribological performance and reliability [1]. In electric vehicles there is growing concern about the performance and reliability of mechanical components such as rolling element bearings and gears [2, 3]. This is due to not only increased temperature and speed expectations, but also because of potential damaging electric currents flowing across the surfaces [4–6]. These electrically induced bearing failures have also been widely observed in wind turbine bearings [7]. Stray electric currents and charges can

build in several ways in a vehicle, and can occur in electric vehicles when the inverter converts power from the batteries to the electric motor. Accumulation of a large charge can induce arcing across the lubricating film of a bearing or gear. Arcing yields a plasma that melts and vaporizes the metal surfaces, causing what is termed as electrical discharge machining (EDM) or by others as electrically induced bearing damage (EIBD). As a consequence, small surficial pits form that can lead to noise, surface fatigue, and eventual failure of an operating bearing [8].

In addition to rolling element bearings, electrical arcing damage can also occur in hydrodynamic sliding

* Corresponding author: Robert L. JACKSON, E-mail: jacksr7@auburn.edu

bearings [9]. In 2011, Sunahara et al. [10] performed an interesting experiment on a transparent elasto-hydrodynamic lubrication (EHL) test rig so that the arcing events could be viewed while the film thickness was measured. They coated a non-conductive transparent disk with a layer of conductive chromium to achieve this. However, their observations could differ from results obtained when contacts occur between a steel bearing raceway and steel rolling elements. Several researchers have also found that electrically conductive greases could prevent electrical pitting in bearings [6, 11, 12]. Other recent work suggested that metallic nanoparticles could enhance the performance of lubricated electrical contacts [13, 14]. Subsequently, reviews of the lubricants required for electric vehicles (EV) suggested the use of nanoparticles to improve the electrical, thermal, and tribological properties of the lubricants [15].

Morris et al. [16] recently laid the foundation for a theoretical approach to the problem by predicting the electrostatic charge in an EHL film that can lead to EIBD. Recently numerical models have also been developed to include the non-conductive lubricating film development between rough surfaces in relative motion due to hydrodynamic lift [17, 18].

Bolted electrical contacts may also use conductive greases to improve performance [19, 20]. The continuous supply of power for electrically powered mass transit vehicles, such as trains and buses, is critically dependent on sliding electrical contacts and pantographs [20–22]. Due to the vibratory nature of aircraft, lubricants are often used to reduce fretting and corrosion of electrical contacts [23, 24]. Slip ring brushes in wind turbines, hydro-generators, and vehicles could also benefit from using conductive lubricants [25]. Utilization of these systems is widespread and growing, and therefore the need for improved lubricants that are electrically compatible is increasing in importance [26].

Most recently, Farfan-Carbara et al. [27] studied the influence of electrification on sliding contacts. Their work found that the application of electricity caused significant wear damage, but slightly reduced the friction. In addition, they found that formulated fluids for gears and automatic transmissions performed better than mineral base oil without additives. According to these investigators [27], the increased damage

noticed with mineral base oil resulted from the higher dielectric strength exhibited by this lubricant. Since the dielectric strength is inversely related to conductivity, the observations suggest that lubricants exhibiting higher conductivities could reduce the surface damage derived from electrical discharges.

Grease is also desirable in many applications given that this material is able to reduce the possibility of lubricant leakage [28]. Sanchez Garrido et al. [29] recently investigated the effects of temperature and roughness on grease performance under the conditions experienced by the bearings of electric motors in EV. That work also considered synthetic and mineral base oils thickened by lithium and polyurea, with lithium greases having the best overall performance. However, the extensive use of lithium for battery production has rendered supplies of this element less abundant, which is expected to increase the use of other types of grease thickeners.

Although the main focus of this work is to study nanoparticle laden greases for bearings of automotive rolling elements, the results could also be applied to other important cases such as electrical connectors. This has become increasingly important for electric vehicles where charging ports and many other connectors in the drive system must perform reliably. A seminal review on lubrication in electrical connectors was provided in 1978 by Campbell [30], who noted that additives to the lubricating fluid are often used to enhance performance. For friction and wear, common additive materials are fatty acids, sulfur compounds, solid lubricants, and zinc-dialkyl-dithiophosphate (ZDDP) [31]. Solid materials such as molybdenum disulfide, polytetrafluoroethylene (PTFE), and graphite can sometimes be used in lubricants to reduce friction and wear. However, in many cases these solid lubricants and additives will induce the formation of a non-conductive film between the surfaces [13, 32, 33].

Nanoparticles and lubricants laden with them (i.e. nano-lubricants) have received a great deal of attention due to their unique properties for a wide variety of materials and applications [34, 35]. Nano-lubricants are colloids, or fluids with nano-scale particles suspended in them (See Fig. 1), which have already been shown to have desirable friction and wear performance qualities [34–36]. Some nanoparticles have proven to reduce the coefficient of friction

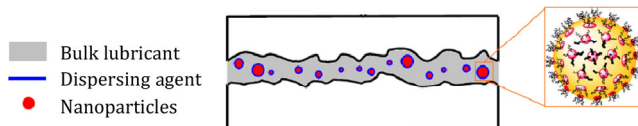


Fig. 1 Schematic of nanoparticle suspension mechanism in a bulk lubricant (base oil).

by 20%–30% [37] and even up to 50% for WS_2 and other nanoparticles [38, 39]. Silver (Ag) nanoparticles have shown to reduce friction by 25%–40% [40–43] and even when added to already fully-formulated lubricants [44]. The preparation of stable dispersions of particles in hydrocarbons has proven to be a difficult task as well [45] because only a few particle stabilizers that dissolve in hydrocarbons are known to be effective at hindering precipitation. Without a stabilizer the particles will also most likely precipitate. While nano-lubricants have shown promising results, quantitative agreement of the available data is missing. This is unsurprising since nano-lubricants are usually prepared via exposing nm-sized particles to some dispersing force, such as mechanical agitation or ultrasound waves. However, the resulting dispersions undergo particle aggregation and precipitation once the dispersing force is no longer applied. Particle precipitation results in not easily reproduced time-dependent properties that are of questionable scientific or practical value. Therefore, the use of a semi-solid, such as grease, is also advantageous in that greases can improve significantly the stability of particle suspensions.

Concentrated Ag colloids (1.3 wt%) were achieved in hydrocarbons containing oleoyl sarcosine (OS) via fast thermolytic reduction of Ag ions at 180 °C [46]. OS served as a surfactant to suspend and stabilize the particles within the hydrocarbons. These spherical colloidal particles with an average diameter of 6 nm were free of precipitation for over 2 years, or after subjecting them to several heating and cooling cycles. An analogous procedure yielded Ag colloids in liquid polyethylene glycol as a solvent consisting of particles with diameter of 7 nm that possess very good lubrication properties [41]. The lubricating properties of this nano-lubricant were studied using the pin on disk method, at different lubrication regimes and across the Stribeck curve. These Ag nanoparticles additives were shown to decrease friction in both the boundary

and elasto-hydrodynamic lubrication regimes [47]. For the previously studied Ag particles the most dominant friction control mechanism was probably the reduction of contact area [48], because energy dispersive X-ray spectroscopy (EDS) measurements demonstrated that no Ag were deposited on the surface.

However, for electrical contacts, the most appealing property of a nano-lubricant (as compared with conventional lubricants) may be an enhanced electrical conductivity. This of course would only be true for a lubricant containing conductive particles. This study therefore focuses on the use of Ag nanoparticles. Even though the contact area is diminished by the particles, the contact resistance is not drastically increased by the presence of the conductive particles. In contrast, many other friction reducing additives such as ZDDP [13] will coat nearly all of the contacts with a non-conductive film [13, 32, 33]. Although the conductivity of a contact lubricated by a fluid containing conductive nanoparticles is not as high as that of pure metallic conductors, in vibrating and sliding electrical contacts the former may show advantageous properties. In these situations, lubricant films or oxide debris can form and the conductive particles might help to bridge across the surfaces or even pierce the non-conductive layer. This suggests that nano-lubricants could be very useful for fretting corrosion and electrical pitting applications, such as for electrical connectors, bearings and brushes used in automotive, and other applications.

More recently, the effect of a lubricant containing different concentrations of Ag particles on electrical contacts was compared with that of a conventional lubricant containing a commercial paraffinic oil [14, 49]. In these tests, the contacts were slid over a range of speeds to capture the behavior for different regimes of lubrication. The change in electrical contact resistance (ECR) determined from measurements performed before and after each test was lower for the nanoparticle-laden lubricant than that of a conventional proprietary lubricant. However, the wear of the samples when employing nanoparticle lubricants was slightly higher than after using the conventional proprietary lubricant. Note that no other additives were present in these nanoparticle lubricants. Therefore, a reasonable assumption is that an optimal

ratio of nanoparticle lubricant with existing additives could yield a superior performance. However, no external electric load was applied in that previous study, and the contacts were sliding instead of rolling as in the current test.

2 Objectives

The current study experimentally investigates the use of lubricating greases consisting of Ag nanoparticles suspended in an alkane and blended into typical electric motor bearing grease formulations. Ag nanoparticles are chosen as one of the additives to be investigated, because they have been previously found to display superior tribological and electrical performances. The effect of different greases with and without Ag nanoparticle additives on the electrical pitting phenomena are evaluated using a rolling element test that features a voltage difference applied across the surfaces. The surficial pitting will be investigated by means of techniques such as profilometry, scanning electron microscope (SEM) and EDS.

3 Methodology

The nanoparticle-laden greases were synthesized by mixing an Ag colloid made in dodecane with professionally prefabricated grease. All the greases considered here are of NLGI 2 consistency and thickened with polyurea. The greases were all based on commercial products provided by Shell [50, 51]. Mineral base grease, synthetic base grease, formulated mineral base grease and formulated synthetic grease were all tested with and without Ag nanoparticles. Note that the synthetic base oil used is poly-alpha-olefin (PAO). Since the Ag nanoparticles were originally suspended in dodecane, grease samples modified only with dodecane were also tested. This procedure yielded twelve different greases to be tested that are listed in Table 1. The blending was conducted using a small-scale mixer/temperature controller and will be described in detail in the following paragraphs. Only small amounts of grease are required for friction and wear testing.

The nanoparticle additives to be tested are Ag colloids (or sols) synthesized in dodecane ($C_{12}H_{26}$) or

eicosane ($C_{20}H_{42}$) according to a procedure developed previously [46]. This method involves the thermal reduction of Ag neodecanoate in either hydrocarbon solvent at 180 °C. Also present in the colloids was OS, consisting of a C_{17} olefinic chain terminated with a carboxylate group able to stabilize Ag particles against precipitation via ionic interaction with the particle surface. The synthesis was performed using an oil bath placed on a hot plate equipped with a thermometer/thermocouple combination to control the temperature. Dodecane containing 0.1 M OS was stirred at 180 rpm with a magnetic stirring bar and heated to 150 °C. After this temperature was reached, enough Ag neodecanoate was quickly added to reach the desired Ag concentration. After complete dissolution of the Ag salt, the temperature was ramped to 180 °C and held constant for 11 min.

Concentrated colloids with a metal mass fraction of up to 1.3% were achieved in $C_{12}H_{26}$ (dodecane). The colloids contained spherical Ag crystallites with an average diameter of 6 nm; in the dodecane system the particles have remained free of precipitation for over 2 years at room temperature. An image of the resulting Ag/dodecane colloid is shown in Fig. S1 in the Electronic Supplementary Material (ESM).

Table 1 List of considered grease samples.

Grease sample description	Abbreviated label
Mineral base grease	min
Mineral base grease with dodecane	Do min
Mineral base grease with 0.19 wt% Ag nanoparticles	NP min
Mineral fully-formulated base grease	FF min
Mineral fully-formulated base grease with dodecane	Do FF min
Mineral fully-formulated base grease with 0.19 wt% Ag nanoparticles	NP FF min
Synthetic PAO base grease	syn
Synthetic PAO base grease with dodecane	Do syn
Synthetic PAO Base Grease with 0.19 wt% Ag nanoparticles	NP syn
Synthetic PAO fully-formulated base grease	FF syn
Synthetic PAO fully-formulated base grease with dodecane	Do FF syn
Synthetic PAO fully-formulated base grease with 0.19 wt% Ag nanoparticles	NP FF syn

Hydrocarbons are miscible with other alkanes at high temperatures, which enables mixing the colloids with base greases under such conditions. Colloids were examined in terms of particle composition via elementary analysis, X-ray diffraction (XRD), tunneling electron microscopy (TEM), and ultraviolet-visible spectroscopy (UV-Vis); spectroscopy; the long-term stability toward precipitation of the sols was also characterized.

Additive packages for lubricating greases are typically mixed into a thickened grease at the end of the processing. As mentioned at the beginning of the section, a similar process was used to incorporate the nanoparticles into existing ‘clean’ greases without other additives. Clean greases without additives (only thickeners and base oil) were used as control samples during the tests. The wear properties of such samples were compared relative to those of ‘clean’ greases with only nanoparticles, a fully formulated grease, and fully-formulated grease with nanoparticles. Greases containing nanoparticles were prepared by mixing 10 g of grease with 2 mL of the previously described colloid solution. The mixing procedure employed pulses generated by a motorized mixer consisting of 15–20 s bursts while applying pressure on the grease between bursts for compaction. All greases were mixed for a minimum of 1 min, and care was taken to homogenize the grease during this process until a uniform product was obtained. A typical image of polyurea greases with and without Ag nanoparticle additives is shown in the ESM as Fig. S2. The resulting Ag nanoparticle laden greases contains approximately 0.19 wt% of Ag. This concentration was chosen since previous work showed success with it in reducing friction and wear, but without a significant electrical load [14].

3.1 Experimental testing

Reciprocating rolling sphere-on-disk (i.e. ball-on-disk) friction tests were performed using a CETR-UMT3 Tribotester (see Fig. 2). An electrical circuit was also secured across the contact as shown in Fig. 3. This circuit allowed for the electrical contact resistance to be measured during the test using an Agilent 34410A multimeter. In this initial study the authors used the simplest setup of a reciprocating motion to avoid

complexities. Few other, if any, existing studies use reciprocating motion, so this work also provides a unique perspective. The reciprocating motion captures the start-stop motion that will occur in real vehicles that other tests do not capture. The reciprocating test was also selected so that the electrical lead contacts were fixed as sliding contacts would introduce noise during the test. A power supply was also connected to the samples in parallel and the voltage through the circuit was set to 31 V. This could be considered a 4-wire resistance test measurement as is common in the electrical contact literature. Utilization of a heating element provided an additional load on the circuit. This results in approximately 0.5 A, or based on the Hertz contact area under 50 N of load, a current flux of 11.1 mA/m². This value is similar to that used by the Southwest Research Institute in cylindrical contact tests [52]. However, the applied electric current

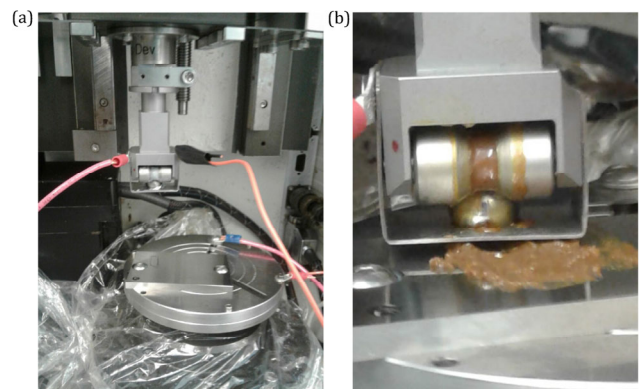


Fig. 2 Photographs of the test setup and fixture (a) before and (b) during testing (when the grease is applied).

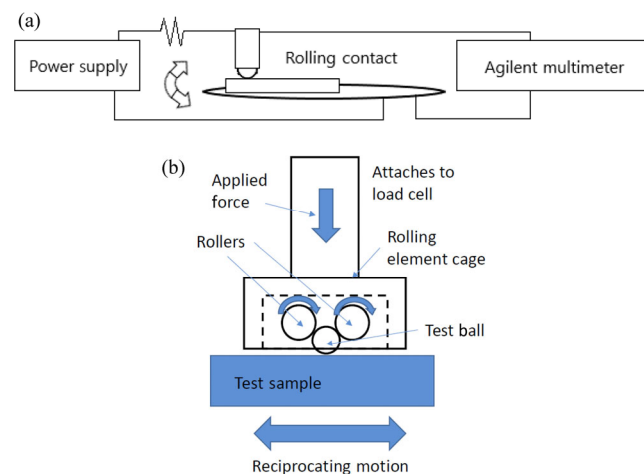


Fig. 3 Schematic of (a) electrical test setup and (b) rolling ball fixture.

and voltage are expected to vary significantly due to changes in the electrical properties across the contact (when the oil film grows or decreases and during arcing).

The load of 50 N is chosen to achieve a Hertz pressure similar to that expected in electric vehicle applications (1.72 GPa). The flat samples were finely ground 52100 steel and loaded against a 3/8" 52100 steel ball. A special roller fixture was used to facilitate rolling of the test balls against the flat steel specimen (see Figs. 2(b) and 3(b)). Greases were applied to all rolling contact surfaces and tests lasted for 1.5 h. The reciprocating tests were run at maximum speed of 1.2 cm/s and an average speed of 0.6 cm/s with a rolling distance of 1 cm. While possible damage of the roller fixture was of concern, no significant problems were encountered during testing.

Using elasto-hydrodynamic theory [53] the current test is expected to operate with a full-film thickness of approximately 30 nm, although it may fluctuate due to the reciprocating motion. Nonetheless, the film thickness will resist compression to a degree (i.e. the squeeze film effect) since the motion does not pause for a substantial amount of time. The nanoparticles are shown to still be influential on friction in the thin film elasto-hydrodynamic regime [47], and may also influence the film thickness.

The testing procedure evaluated four grease types (mineral base, mineral formulated, synthetic base, and synthetic formulated) with and without Ag nanoparticles or dodecane (used to deliver the nanoparticles). Again a list of these considered samples are in Table 1. All these greases complied with the ISO 100 viscosity specifications and used a polyurea grease thickener to achieve a consistency of NLGI 2 (penetration from 265 to 295). No extreme pressure (EP) additives are present in any of the greases. The finished greases are lubricating materials currently manufactured for industrial use and contain additives that protect them from oxidation and corrosion. The base grease was obtained by removing samples from the manufacturing process before the introduction of additives.

Each experiment was replicated three times, always using a fresh surface and new ball, which resulted in 36 separate tests. A limited selection of tests was also run with no electrical load (without any applied voltage

or current). Such tests resulted in no measurable wear and confirmed that the damage was dominantly produced by the applied electrical load (see Fig. 4).

4 Results and discussion

After testing was completed, the samples were characterized using optical microscopy, stylus profilometry, SEM, and EDS. Presented in Fig. 4 are optical microscopy images of surfaces: (a) before an experiment, (b) a test without any electrical load, and (c) in the presence of an electrical current. The tests were performed with surfaces covered with mineral oil polyurea grease, which was removed prior to imaging. As shown by the images, a clear wear track was noticed only in the experiment performed under an electrical load. This wear track was confined to the region between the starting point of the run and the end point where the direction of rolling was reversed. The wear track became visible because of differences in light reflection between the area containing pitting, deposited metal and the pristine steel surface. Elevated carbon on the wear track may have also played a role. Additional SEM images revealed that metal pitting took place mainly in the locations where rolling started and then changed direction, Fig. 4(d) is a representative example. Evidence that the wear track originated from deposition of metal ablated from the start and end regions of the run is shown in Fig. 4(e). A thorough analysis of the SEM results will be presented later. Note that the test setup also enabled recording of the lateral or friction force. However, since the contacts are rolling there was no measurable difference in the lateral forces between different greases.

Shown in Fig. 5 are SEM results acquired from an experiment in the presence of an electrical load using mineral grease with dodecane but without Ag particles. The top left image demonstrates that substantial pitting occurred on the surface of the substrate. Also included in Fig. 5 are EDS maps showing the distribution of Cr, Mn, Fe, C, and O within the same area. Analysis of the EDS maps indicated that the distribution of Cr, Mn, and Fe remained unchanged; C and O signals were detected only in samples that experienced arcing. No Ag was observed on the surfaces. Figure 6 resulted from an overlay of the distribution maps (excluding the Cr data) and

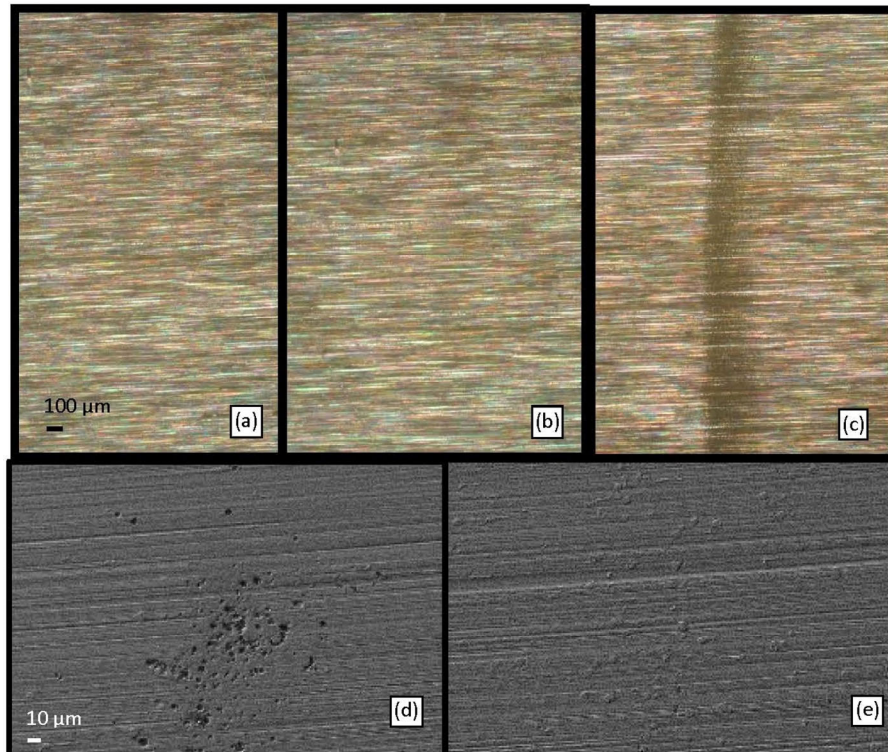


Fig. 4 Optical microscopy images of surfaces (a) before a run, (b) after an experiment without electric current, and (c) worn in the presence of an electric load. Also included are SEM images of (d) a surface after an electric test showing arc pitting, and (e) redeposition of ablated metal on the steel.

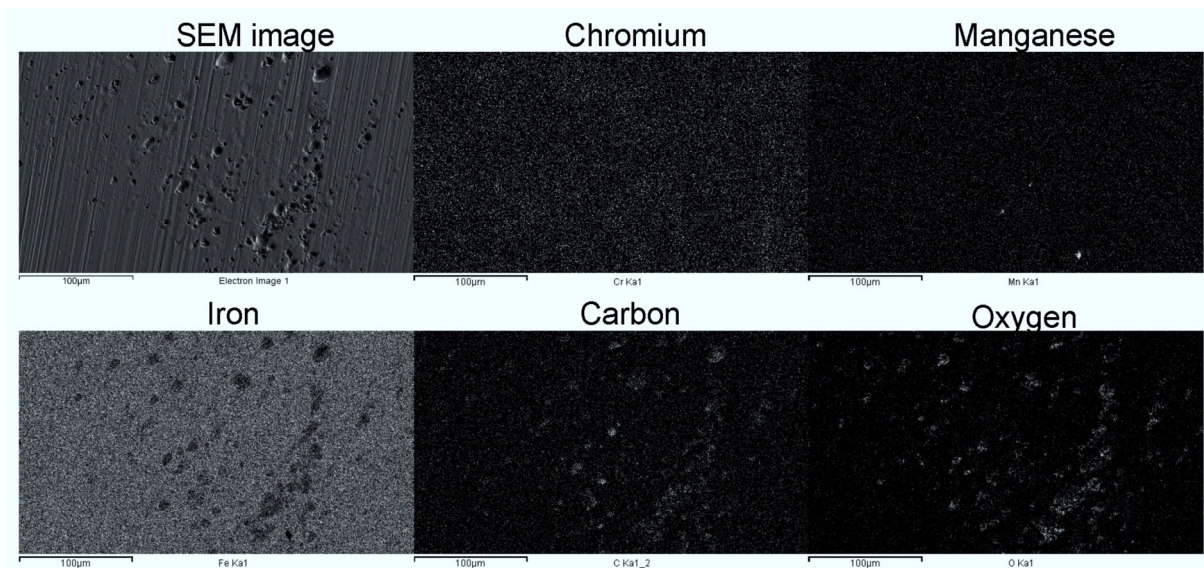


Fig. 5 SEM and EDS images of a worn surface region. Mineral grease containing dodecane but without Ag particles served as the lubricant. The scale bar included on the bottom left of each image corresponds to 100 μm .

demonstrated that O and C were present mostly within the pits. These observations suggest that arcing produced the pitting and chemically degraded the grease in these locations.

Grease samples were also collected after the tests and examined using Fourier transform infrared spectroscopy (FTIR) to check for this degradation. However, no measurable differences were observed.

This is probably due to the micrometer-scale contact patch containing a small amount of grease that is too diluted in the grease sample.

Analysis of the wear tracks shown in the SEM images (see Figs. 7–10) revealed that not only are there quantitative differences in the number of pits detected in tests with different greases, but that a larger

number of pits were present at the starting and end points of the wear tracks. The track is the area over which the ball rolls and at the end point the direction of rolling is reversed after a short pause. Several reasons could account for such behavior. At the track end the film thickness should be at a minimum as the surfaces momentarily lose EHL and come closer together. In

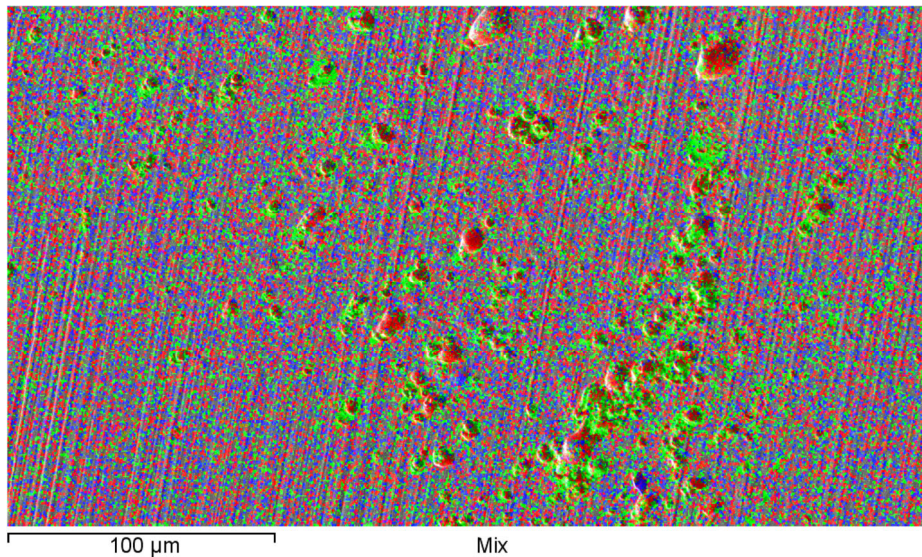


Fig. 6 An overlay image of the EDS maps for C–Red, O–Green, Fe–Blue, and Mn–Orange. The Cr map was excluded to improve the clarity of presentation.

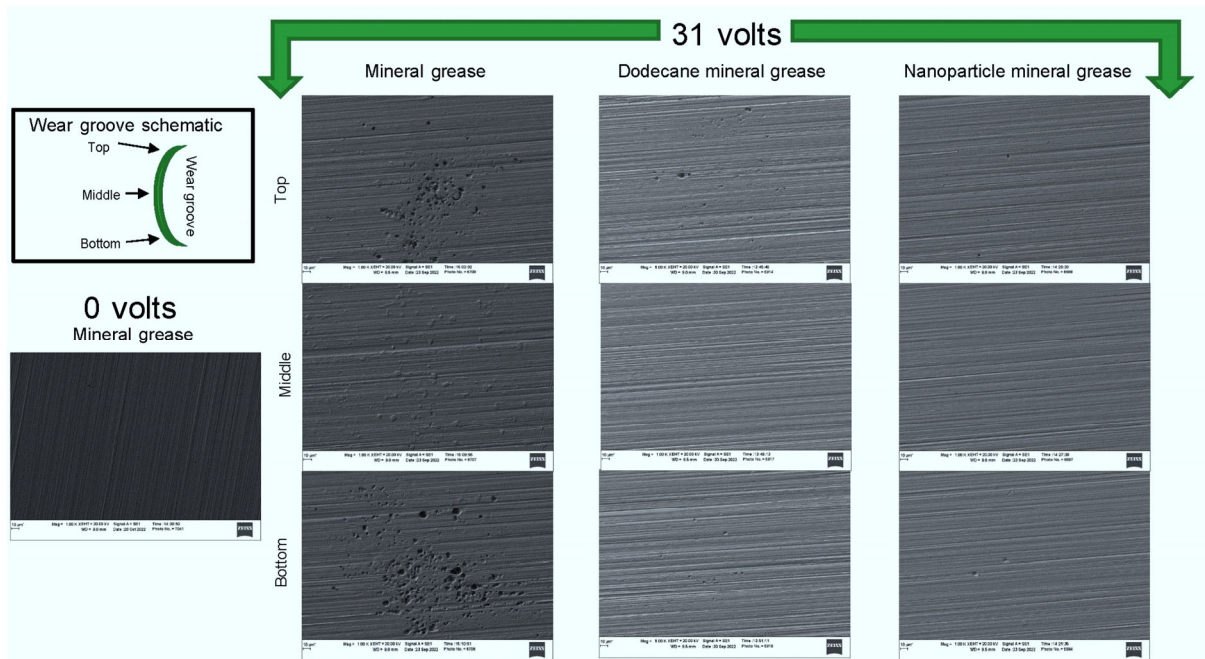


Fig. 7 SEM image of electrically pitted substrates, experiments conducted with mineral grease samples. Left top scheme labelled “Wear groove schematic”: representation of a wear groove on the steel substrate, the top and bottom labels indicate the points at which the ball motion is reversed, middle label marks area of highest metal deposition.

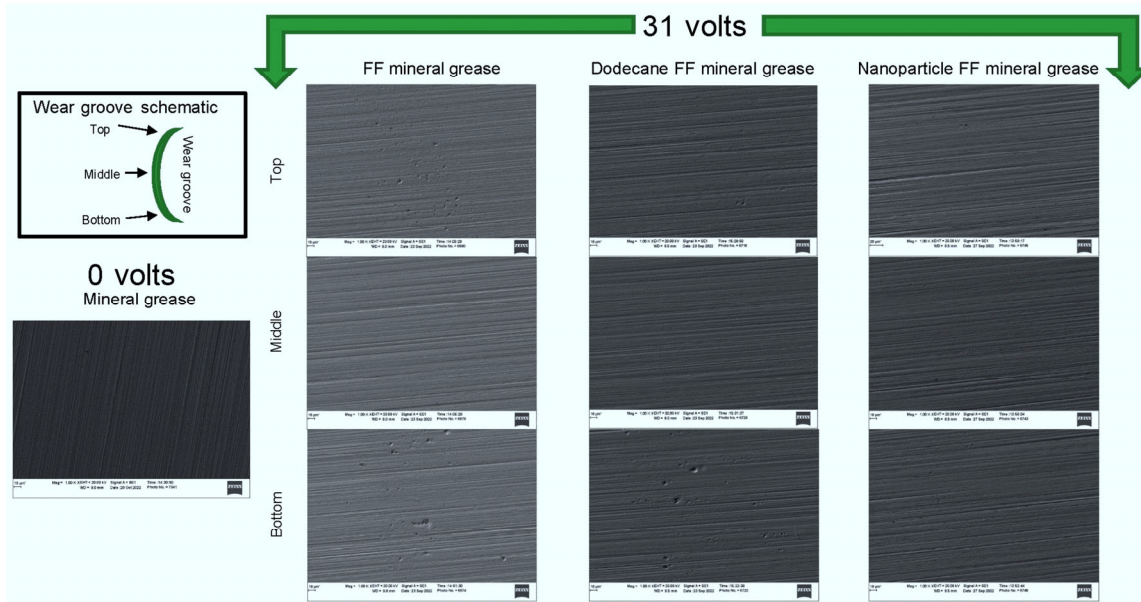


Fig. 8 SEM image of electrically pitted substrates, experiments conducted with fully-formulated mineral grease samples. See Fig. 7 for additional details.

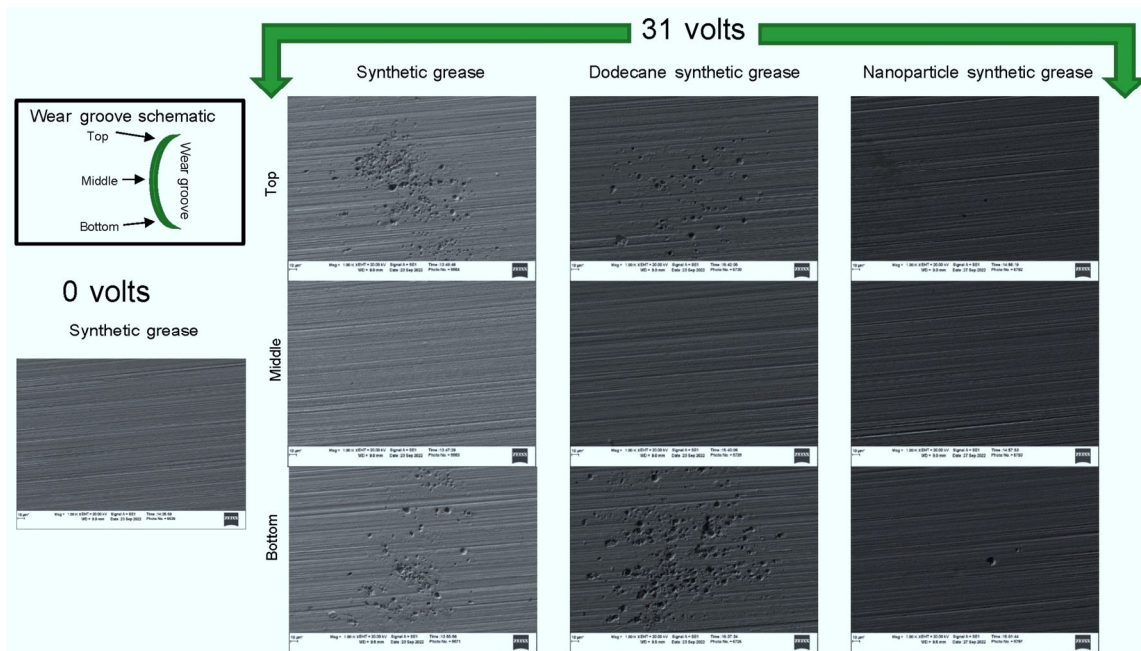


Fig. 9 Image analysis of SEM of electrically pitted substrates, experiments conducted with synthetic grease samples. See Fig. 7 for additional details.

addition, if the arcing is the result of a build up of charge at the asperities on the surfaces, perhaps the charge has more time to grow as the surface motion slows and pauses. As is also evident from Figs. 7–10, pitting obtained with greases containing nanoparticles (Ag dodecane colloid), and sometimes with just dodecane, is less extensive than the damage noticed

with the grease. In addition, the fully formulated greases appear to inhibit pitting more efficiently than the clean greases without additives. The goal of the next part is to extract a more quantitative analysis of the SEM observations.

Quantitative information about the damage resulting from surface pitting was obtained via analysis of the

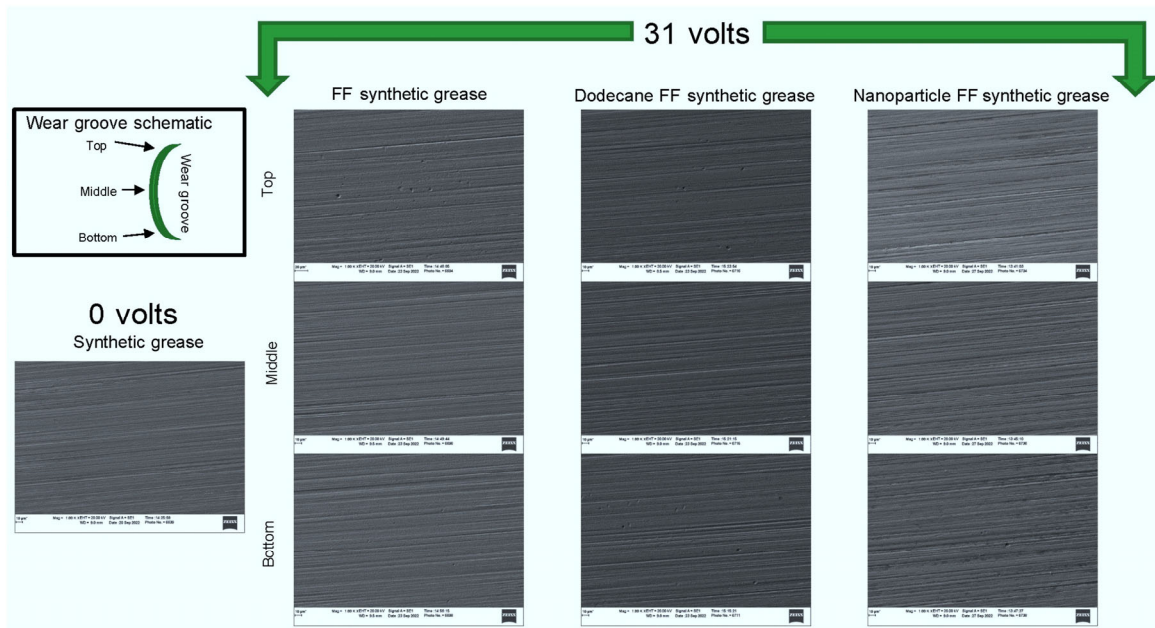


Fig. 10 SEM image of electrically pitted substrates, experiments conducted with fully-formulated (FF) synthetic grease samples. See Fig. 7 for additional details.

SEM images using the software ImageJ. The procedure consisted of first identifying the eroded places followed by summation of the surface area of those eroded places. Figure 11 depicts a graphical representation of the image analysis for an experiment that employed a mineral grease sample. The eroded areas are identified by yellow borders. In all tests, the images obtained at both ends of the wear tracks were analyzed using the same scale and methodology. Such analysis yielded a percentage of surface damage for each of the different greases at the end of the resulting wear groove. Since

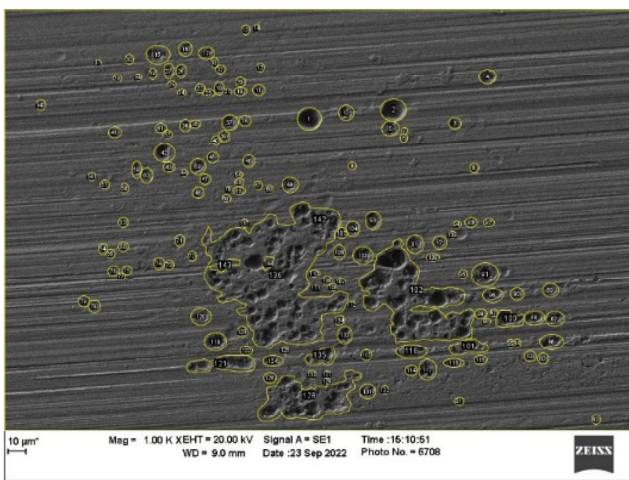


Fig. 11 Image analysis representation of a flat substrate tested with mineral grease as a lubricant.

only the ends of the wear grooves are considered, this procedure does not represent the percentage of surface damage across an entire wear track.

Plotted in Fig. 12 are the results obtained by analysis of the images illustrating the damage of the substrates derived from electrical pitting of the surface. First,

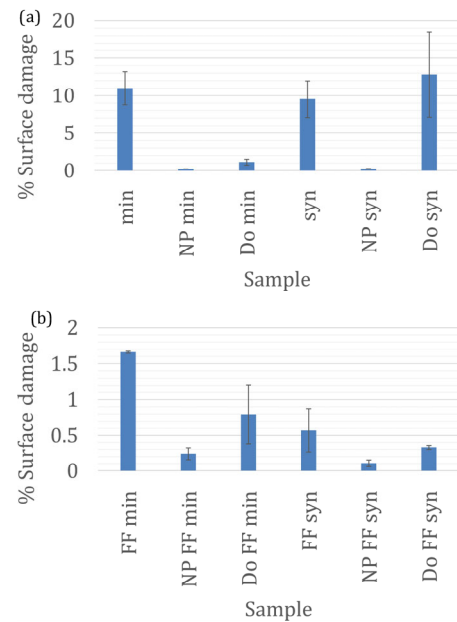


Fig. 12 Percentage of surface damage for flat substrates in tests with different samples when different greases. Panel (a) depicts the results for the base greases, presented in panel (b) are the data for the fully formulated greases.

the image analysis clearly indicated that the highest surface damage induced by electrical pitting took place in experiments that employed unmodified or clean synthetic and mineral greases (Fig. 12(a)). Tests run with synthetic grease mixed with dodecane also yielded a larger percentage of surface damage. It is clear from Fig. 12(a) that the addition of the silver nanoparticles solution to the base greases drastically reduced the surface damage on the samples. Figure 12(b) depicts the results for the fully formulated greases that included antioxidants and anti-corrosion additives. Although the additives in the fully formulated oils do appear to reduce the surface damage, the nanoparticles further reduce it beyond the conventional additive formulation alone. Experiments with the four greases containing Ag nanoparticles (dodecane colloid) yielded the lowest percentages of surface damage, supporting earlier conclusions. Furthermore, most experiments with dodecane and fully formulated greases yielded less surface damage as compared to tests with unmodified greases, but in differing degrees.

Next, a stylus profilometer with a 2 μm tip was used to measure all the wear grooves. As illustrated in Fig. 13, circular shaped pits analogous to those shown in Figs. 4(d) and 5(a) were detected by means of profilometry. However, the damage was not usually present as a defined or continuous wear groove, so wear rate, wear groove width, or wear volume were not evaluated. The trends are not as pronounced as the SEM image analysis results. This is due to the damage on the track not only being represented by

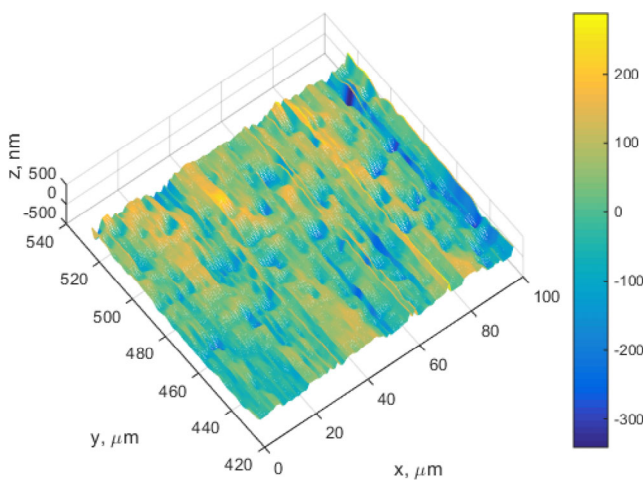


Fig. 13 Profilometer data obtained in an experiment conducted under electrical load on surfaces lubricated using a mineral grease.

pitting, but also by raised peaks of redeposited debris (recall the discussion about Figs. 4(d) and 4(e)). The profilometry does provide some quantitative dimensions to the pits. They appear to be on the order of 200 nm deep and a few micrometers across.

Measurements of the electrical resistance across the contact during testing were conducted as well. Even though the electrical contacts of the leads were made static due to the reciprocating nature of the experiments, significant fluctuations in the data derived from tests were still observed. Note that each point in the plot represents the average resistance measured at 50 Hz during 1 s. Large fluctuations were observed probably because the circuit includes several other moving contacts, such as the roller fixture. The roughness of the surfaces and changes in local grease film thickness could have also contributed to the large dispersion of the resistance data. Finally, arcing or EDM events themselves may constitute another possible factor contributing to the observed resistance fluctuations. Obviously, the resistance increases drastically at the initiation of motion between the surfaces. This is probably due to the formation of a film between the surfaces containing less conductive grease as predicted by theoretically models [17].

The measured electrical contact resistance over the duration of each test was averaged for each type of grease and is presented in Fig. 14. As mentioned previously, this observable was defined as ECR, although this quantity also includes other contributions from the wire, lead contacts, etc. Nonetheless, a

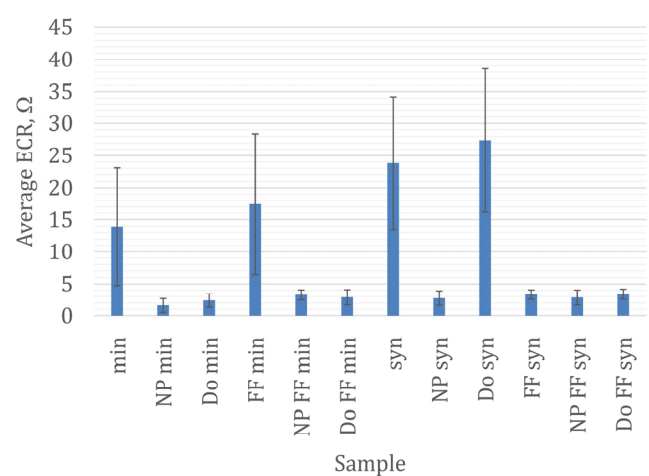


Fig. 14 Averaged ECR obtained from the three tests conducted for each grease sample.

comparison of these averages show that the nanoparticles yielded an overall lower ECR as compared to the other greases. Fully formulated greases and also those modified with dodecane also showed a decrease in ECR, but consistency was lacking across all samples. A lower ECR value may suggest a mechanism in which greases containing Ag nanoparticles reduce the surface pitting damage. In theory the particles may provide a shorter path for the electrical current to cross the relatively non-conductive lubricant thereby inhibiting arc formation. Decreasing the path distance could also reduce the size of the arc.

The initiation of arcing across the film can be approximately predicted by the dielectric strength. The dielectric breakdown strength of mineral oil is approximately 10–15 mV/m [54]. If the voltage across a film exceeds this, the electrons may overcome the insulation of the film by breaking it down into a plasma, which disassociates the electrons and facilitates conduction. Usually this requires high voltage and results in high temperatures, causing damage to the surfaces. The thickness of the film multiplied by the dielectric strength predicts this voltage, also known as the dielectric voltage. Therefore, a smaller film requires less voltage to arc across. Following established elasto-hydrodynamic lubrication theory [55] the film thickness in the current experiments is approximately 30 nm. Note that this thickness will vary based on the roughness and the reciprocating motion. Then the dielectric voltage is on the order of single volts.

Now consider if conductive silver nanoparticles are dispersed within the film. In the current work the particle density, n , is 9.1×10^{21} particles/m³. The Wigner–Sietz radius [56] is an approximation of the average distance between the center of the particles:

$$r = \sqrt[3]{\frac{3}{4\pi n}} \quad (1)$$

Equation (1) predicts an average distance between the silver nanoparticles of 29.7 nm. Considering that the nanoparticles are 6 nm in diameter, the distance between the surfaces of the particles is approximately 23.7 nm, which is less than the film thickness. The authors propose that this might allow the electric current to conduct across the films at lower voltages

which may result in less damaging arcs. In addition, the nanoparticles might agglomerate and pass between the surfaces providing even shorter distances for the electrons to cross.

5 Conclusions

This work first demonstrated the erosive effect induced by the flow of an electrical current across a greased rolling contact. Electrical current increased the wear on the contacts measurably as compared to the erosion noted in conventional rolling, that is, without current. The damage came in the form of pits believed to be the result of micro-scale arcs occurring between the surfaces and across the film of lubrication. Scanning electron microscopy (SEM)/energy dispersive spectroscopy (EDS) findings showed that surface erosion was concentrated at the points of the wear track where rolling of the steel ball reversed direction. In addition, some of the eroded metal was deposited in the mid-region of the wear track, away from the turning points. This observation suggests that the greases transported the eroded metal to the places where deposition occurred. Furthermore, the formed surface pits contained carbon and oxygen implying that chemical decomposition of the greases took place due to micro-scale arcing.

Greases with Ag nanoparticles decrease the surface pitting damage as compared to all other lubricants tested. This conclusion is supported by the SEM image analysis. Fully-formulated greases as well as greases with dodecane also showed an improvement. While no drastic changes in the average electrical contact resistance were noticed, the electrical contact resistance (ECR) values appear to decrease for greases with nanoparticles. Note that in previous tests the Ag nano-lubricant yielded lower friction coefficients and less wear as compared to many conventional lubricants.

One possible mechanism involves a change in the electrical conductivity of the grease, but some additives could also alter the rheology and facilitate changes in the film thickness between the surfaces. However, previous studies showed that the addition of similar concentrations of nanoparticles to oils induced relatively little change in viscosity. This work also

proposes that the particles decrease the distances between conductive surfaces thereby lowering the voltage needed to cross the film, and thereby decreasing the damage of the arcs. The mechanisms by which greases containing Ag nanoparticles reduce the pitting induced by arcing remain unconfirmed, but further studies are planned to elucidate this phenomenon. This is also true for the benefits sometimes observed for dodecane and fully formulated greases.

Acknowledgements

The authors thank NLGI for funding this project via the Academic Outreach-Research Grant, Shell for providing grease samples, the Timken Company for providing flat samples of 52100 steel, and Bruker Nano Surfaces for providing the rolling element test fixtures. We also appreciate the guidance of Dwayne (Greg) MORRIS of Shell throughout the project, and the help of Mike Miller during scanning electron microscopy (SEM) determinations. Thanks to Hamed GHAEDNIA for his creation of Fig. 1 and other discussions about nanoparticle lubrication over the years.

Declaration of competing interest

The authors have no competing interests to declare that are relevant to the content of this article.

Electronic Supplementary Material: Supplementary material is available in the online version of this article at <https://doi.org/10.1007/10.1007/s40544-023-0837-4>.

Open Access This article is licensed under a Creative Commons Attribution 4.0 International License, which permits use, sharing, adaptation, distribution and reproduction in any medium or format, as long as you give appropriate credit to the original author(s) and the source, provide a link to the Creative Commons licence, and indicate if changes were made.

The images or other third party material in this article are included in the article's Creative Commons licence, unless indicated otherwise in a credit line to the material. If material is not included in the article's Creative Commons licence and your intended use is

not permitted by statutory regulation or exceeds the permitted use, you will need to obtain permission directly from the copyright holder.

To view a copy of this licence, visit <http://creativecommons.org/licenses/by/4.0/>.

References

- [1] Holmberg K, Erdemir A. The impact of tribology on energy use and CO₂ emission globally and in combustion engine and electric cars. *Tribol Int* **135**: 389–396 (2019)
- [2] Farfan-Cabrera L I. Tribology of electric vehicles: A review of critical components, current state and future improvement trends. *Tribol Int* **138**: 473–486 (2019)
- [3] Shah R, Gashi B, González-Poggini S, Colet-Lagrille M, Rosenkranz A. Recent trends in batteries and lubricants for electric vehicles. *Adv Mech Eng* **13**(5): 168781402110217 (2021)
- [4] Kudelina K, Asad B, Vaimann T, Belahcen A, Rassölkin A, Kallaste A, Lukichev D V. Bearing fault analysis of BLDC motor for electric scooter application. *Designs* **4**(4): 42 (2020)
- [5] Prasad S, Krishnanunni S. Review on analysis of failures modes in the electric vehicles due to electric bearings. *Int Res J Eng Technol* **7**(12): 1722–1725 (2020)
- [6] He F, Xie G X, Luo J B. Electrical bearing failures in electric vehicles. *Friction* **8**(1): 4–28 (2020)
- [7] Liu Z P, Zhang L. A review of failure modes, condition monitoring and fault diagnosis methods for large-scale wind turbine bearings. *Measurement* **149**: 107002 (2020)
- [8] Raadni S, Kleesuwan S. Electrical pitting wear debris analysis of grease-lubricated rolling element bearings. *Wear* **271**(9–10): 1707–1718 (2011)
- [9] Chatterton S, Pennacchi P, Vania A. Electrical pitting of tilting-pad thrust bearings: Modelling and experimental evidence. *Tribol Int* **103**: 475–486 (2016)
- [10] Sunahara K, Ishida Y, Yamashita S, Yamamoto M, Nishikawa H, Matsuda K, Kaneta M. Preliminary measurements of electrical micropitting in grease-lubricated point contacts. *Tribol Trans* **54**(5): 730–735 (2011)
- [11] Suzumura J. Prevention of electrical pitting on rolling bearings by electrically conductive grease. *QR RTRI* **57**(1): 42–47 (2016)
- [12] Chen Y, Jha S, Raut A, Zhang W Y, Liang H. Performance characteristics of lubricants in electric and hybrid vehicles: A review of current and future needs. *Front Mech Eng* **6**: 571464 (2020)

- [13] Jackson R L, Coker A B, Tucker Z, Hossain M S, Mills G. An investigation of silver-nanoparticle-laden lubricants for electrical contacts. *IEEE Trans Compon Packag Manuf Technol* **9**(2): 193–200 (2019)
- [14] Crilly L, Jackson R L, Mills G, Bond S, Bhargava S. An exploration of the friction, wear, and electrical effects of nanoparticle enhanced and conventional lubricants. *IEEE Trans Compon Packag Manuf Technol* **12**(11): 1757–1770 (2022)
- [15] Shah R, Gashi B, Rosenkranz A. Latest developments in designing advanced lubricants and greases for electric vehicles—An overview. *Lubr Sci* **34**(8): 515–526 (2022)
- [16] Morris S A, Leighton M, Morris N J. Electrical field strength in rough infinite line contact elastohydrodynamic conjunctions. *Lubricants* **10**(5): 87 (2022)
- [17] Jackson R L, Angadi S. Modelling of lubricated electrical contacts. *Lubricants* **10**(3): 32 (2022)
- [18] Jackson R L, Angadi S. Electrical contact during a rolling vibratory motion considering mixed lubrication. *J Tribol* **145**(8): 082201 (2023)
- [19] Gatherer J, Jackson R L. A multi-variable parametric study on the performance of bolted busbar contacts. In *Proceedings of 2015 IEEE 61st Holm Conference on Electrical Contacts (Holm)*. October 11–14, 2015, San Diego, CA, USA. IEEE, 124–131.
- [20] Chudnovsky, B H. *Lubrication of Electrical and Mechanical Components in Electric Power Equipment*. Boca Raton, FL (USA): CRC Press, 2019.
- [21] Song Y, Ouyang H J, Liu Z G, Mei G M, Wang H R, Lu X B. Active control of contact force for high-speed railway pantograph-catenary based on multi-body pantograph model. *Mech Mach Theory* **115**: 35–59 (2017)
- [22] Wu G N, Gao G Q, Wei W F, Yang Z F. Electric Contact Material of Pantograph and Catenary. In *Proceedings of The Electrical Contact of the Pantograph-Catenary System*. Singapore: Springer, 2019: 195–220.
- [23] Slade P G. *Electrical Contacts: Principles and Applications*. 2nd ed. Boca Raton, FL: CRC Press, 2014.
- [24] Abbott, W. H. Performance of the gold-tin connector interface in a flight environment. In: *Proceedings of the Forty-Fourth IEEE Holm Conference on Electrical Contacts*, Arlington, VA, 1998: 141–150.
- [25] Fu Y, Qin H L, Xu X, Zhang X L, Guo Z G. The effect of surface texture and conductive grease filling on the tribological properties and electrical conductivity of carbon brushes. *Tribol Int* **153**: 106637 (2021)
- [26] Larsson E, Andersson A M, Kassman Rudolphi Å. Grease lubricated fretting of silver coated copper electrical contacts. *Wear* **376**: 634–642 (2017)
- [27] Farfan-Cabrera L I, Erdemir A, Cao-Romero-Gallegos J A, Alam I, Lee S. Electrification effects on dry and lubricated sliding wear of bearing steel interfaces. *Wear* **516**: 204592 (2023)
- [28] Hemanth G, Suresha B, Ananthapadmanabha. Hybrid and electric vehicle tribology: A review. *Surf Topogr: Metrol Prop* **9**(4): 043001 (2021)
- [29] Sanchez Garrido D, Leventini S, Martini A. Effect of temperature and surface roughness on the tribological behavior of electric motor greases for hybrid bearing materials. *Lubricants* **9**(6): 59 (2021)
- [30] Campbell W. The lubrication of electrical contacts. *IEEE Trans Compon Hybrids Manuf Technol* **1**(1): 4–16 (1978)
- [31] Rudnick, L R. *Lubricant Additives: Chemistry and Applications*. Boca Raton, FL (USA): CRC press, 2009.
- [32] Bakunin V N, Kuzmina G N, Kasrai M, Parenago O P, Bancroft G M. Tribological behavior and tribofilm composition in lubricated systems containing surface-capped molybdenum sulfide nanoparticles. *Tribol Lett* **22**(3): 289–296 (2006)
- [33] Zhang M, Wang X B, Fu X S, Xia Y Q. Performance and anti-wear mechanism of CaCO₃ nanoparticles as a green additive in poly-alpha-olefin. *Tribol Int* **42**(7): 1029–1039 (2009)
- [34] Menezes, P L., Nosonovsky, M, Ingole, S P, Kailas, S V, and Lovell, M R. *Tribology for Scientists and Engineers*. New York: Springer, 2013.
- [35] Htwe Y Z N, Al-Janabi A S, Wadzer Y, Mamat H. Review of tribological properties of nanoparticle-based lubricants and their hybrids and composites. *Friction* **12**(4): 1–22 (2023)
- [36] Singh A, Chauhan P, Mamatha T G. A review on tribological performance of lubricants with nanoparticles additives. *Mater Today Proc* **25**: 586–591 (2020)
- [37] Ghaednia H, Jackson R L, Khodadadi J M. Experimental analysis of stable CuO nanoparticle enhanced lubricants. *J Exp Nanosci* **10**(1): 1–18 (2015)
- [38] Greenberg R, Halperin G, Etsion I, Tenne R. The effect of WS₂ nanoparticles on friction reduction in various lubrication regimes. *Tribol Lett* **17**(2): 179–186 (2004)
- [39] Thampi A D, Prasanth M A, Anandu A P, Sneha E, Sasidharan B, Rani S. The effect of nanoparticle additives on the tribological properties of various lubricating oils—Review. *Mater Today Proc* **47**: 4919–4924 (2021)
- [40] Ghaednia H, Hossain M S, Jackson R. Tribological performance of silver nanoparticle-enhanced polyethylene glycol lubricants. *Tribol Trans* **59**: 585–592 (2016)
- [41] Ghaednia H, Hossain M S, Jackson R L. Tribological performance of silver nanoparticle-enhanced polyethylene glycol lubricants. *Tribol Trans* **59**(4): 585–592 (2016)

- [42] Kumara C, Luo H M, Leonard D N, Meyer H M, Qu J. Organic-modified silver nanoparticles as lubricant additives. *ACS Appl Mater Interfaces* **9**(42): 37227–37237 (2017)
- [43] Chinnachamy R, Durairaj V, Saravanamuthu M, Rajagopal V. Evaluation of the effect of silver nanoparticles on the tribological and thermophysical properties of bio-lubricants. *Proc Inst Mech Eng E J Process Mech Eng* **237**(2): 410–417 (2023)
- [44] Ghaednia, H. An analytical and experimental investigation of nanoparticle lubricants, Ph.D. Thesis, Auburn, AL (USA): Auburn University, 2014.
- [45] Azman N F, Samion S. Dispersion stability and lubrication mechanism of nanolubricants: A review. *Int J Precis Eng Manuf Green Technol* **6**(2): 393–414 (2019)
- [46] Darvin J R, Hossain M S, Nabil M, Uertz J, Mills G. Concentrated Ag nanoparticles in dodecane as phase change materials for thermal energy storage. *ACS Appl Nano Mater* **2**(10): 6187–6196 (2019)
- [47] Ghaednia H, Babaei H, Jackson R L, Bozack M J, Khodadadi J M. The effect of nanoparticles on thin film elasto-hydrodynamic lubrication. *Appl Phys Lett* **103**(26): 263111-1–263111-5 (2013)
- [48] Ghaednia H, Jackson R L. The effect of nanoparticles on the real area of contact, friction, and wear. *J Tribol* **135**(4): 041603 (2013)
- [49] Crilly L, Jackson R L, Bond S, Mills G, Bhargava S. An investigation of the electrical contact resistance change, lubrication, and wear properties of a nanolubricant. In *Proceedings of the IEEE 66th Holm Conference on Electrical Contacts and Intensive Course*. San Antonio, TX (USA). 2020: 1–7.
- [50] Technical Data Sheet: Shell Gadus S3 T100 2 2021. Available from: <https://shell-livedocs.com/data/published/en-US/345773ce-520f-4d65-9bbf-d73b1ec646d8.pdf>.
- [51] Technical Data Sheet: Shell Gadus S5 T100 2. 2016. Available from: https://www.powerlubeind.com/sites/default/files/default_images/downloads/lubricant_specifications/tds/shell/shell_gadus_s5_t100_2_tds.pdf.
- [52] Lee P M, Sanchez C, Frazier C, Velasquez A, Kostan T. Tribological evaluation of electric vehicle driveline lubricants in an electrified environment. *Frontiers in Mechanical Engineering*, in press, DOI 10.3389/fmech.2023.1215352.
- [53] Cheng H S. Discussion: “Isothermal elasto-hydrodynamic lubrication of point contacts: Part 1—Theoretical formulation” *J Lubr Technol* **98**(2): 228 (1976)
- [54] Lide D R. CRC Handbook of Chemistry and Physics, 3rd electronic ed. Boca Raton, FL (USA): CRC Press, 2000.
- [55] Hamrock B J, Schmid S R, Jacobson B O. Fundamentals of Fluid Film Lubrication. Boca Raton, FL (USA): CRC Press, 2004.
- [56] Girifalco L A. *Statistical Mechanics of Solids*. Oxford: Oxford University Press, 2000.



Samuel BOND. He received his bachelor degree in chemistry in 2012 from Winthrop University, Rock Hill, South Carolina. After that, he was a technical associate in the Polymeric Colorants and Ingredients

group at Milliken & Company. Currently, he is a Ph.D. student in the Dr. MILLS Lab of Chemistry at Auburn University, Auburn, Alabama. His research interests include photosensitive polymeric systems and nanoparticle synthesis.



Robert L. JACKSON. He is a professor of mechanical engineering at Auburn University. He received his B.S., M.S., and Ph.D. degrees from the Georgia Institute of Technology. After completing his Ph.D. in 2004, he joined the faculty of Auburn University. In 2012, Prof. JACKSON also

initiated one of the first undergraduate minors in the field of tribology. He is an American Society of Mechanical Engineers (ASME) and Society of Tribologist and Lubrication Engineers (STLE) Fellow and has published over 100 journal papers. His research interests include contact mechanics, hydrodynamic lubrication, lubricant additives, electrical contacts, and machine component design.



German MILLS. He completed his Licenciado degree in chemistry from the University of Santiago, Chile in 1981, and a Ph.D. in physical chemistry from the Technical University of West Berlin, Germany, in 1985. From 1985 to 1987 he was a post-doctoral fellow at Argonne National Laboratory, followed by a Research Fellow

position at the California Institute of Technology between 1987 and 1989. He then joined the Department of Chemistry of Auburn University as an assistant professor and rose through the ranks to professor. His publications have been centered on mechanisms of nanoparticle formation, polymer and semiconductor photochemistry, as well as responsive materials. Dr. MILLS is a member of the American Chemical Society.